COBEM 2021 26th International Congress of Mechanical Engineering
ABCM Associação Brasileira de Engenharia e Ciências Mecânicas
November 22-26, 2021, Virtual Congress, Brazil

COB-2021-0054
HIGH ORDER IMMERSED INTERFACE METHOD FOR COMPRESSIBLE INVISCID FLOWS

L. P. Velandia*
lpvelandial@usp.br
J. Solarte-Pineda
jsp@sc.usp.br
P. C. Greco Jr*
pgreco@sc.usp.br
São Carlos School of Engineering (EESC), University of São Paulo (USP).
Avenue Trabalhador são-carlense, 400 - ZIP 13566-590 - São Carlos - Brazil

Abstract. *In this paper, a high order immersed interface boundary method for compressible flow is presented, fourth order of precision in both space and time is achieved using the classic Runge Kutta method and a compact finite difference method respectively. Close to the interface, where the flow properties are discontinuous, the central finite difference scheme is changed in favor of preserving the order of precision of the compact scheme. The verification process is carried, using the advection diffusion equation in one dimension also the compressible flow over a flat plate is used in order to validate the code.*

Keywords: *Immersed boundary method, CFD, compact finite difference,inviscid flow*

1. INTRODUCTION

Fluid structure-iteration methods, as the Immersed Boundary Method (IBM) has been applied and tested successfully in the last few decades. Those methods arise as an alternative solution to simulate complex geometries without using body conforming algorithms, Peskin (2003), Peskin (1977) introduce the IBM in the late 70s. Subsequently, several methods arise in order to compute the external force. For instance, Goldstein *et al.* (1993) and Sciences (1996) use an iterative damped function to apply the internal boundary condition. Mohd-yusof (1997) introduced a different approach to compute the boundary condition known as direct forcing method and solve the incompressible Navier-Stokes equations, Solarte-Pineda and Greco (2016) use a similar approach solving the compressible Euler equations. The Immersed Interface Method (IIM) is an IBM based method, which has the advantage of keeping the order of accuracy at the interface through the use of a jump function, although in literature some methods do not use jump condition. The IBMs and the IIMs can identify sharp interfaces accurately and capture discontinuities relatively easy. In the IIM, the key idea is that the differentiation scheme is modified at the interface between the fluid and the body in order to maintain the order of precision. This method was first introduced by Xu (2011) and Lai and Li (1999). Xu (2011) were the first in modifying a central finite difference stencil over a discontinuity in order to maintain second order of accuracy. They compared his method, with the discrete delta function approach from Peskin, and show that this IIM has a second order of accuracy in the whole domain, even in the interface in contrast with the Peskin approach. While Lai and Li (1999) present a formulation for generating a jump condition function type to solve the Navier Stokes equations of a three-dimensional flow, for moving membranes. Some author combines both the IBM and the IIM to improve the results as: Hossan *et al.* (2014), Hu *et al.* (2015). Li and Ito (2006), wrote a book concerning of the IIM to solve elliptic interface problems. In physics a considerable number of problems require the application of high order of accuracy methods, for example: Linnick and Fasel (2005) present a fourth order of accuracy IIM using the stream function formulation to solve the incompressible Navier Stokes equation, Hosseinverdi and Fasel reaches seventh order for the first derivative and sixth for the second derivative of the incompressible Navier Stokes equations, Marichal *et al.* (2016) use a particle to mesh interpolation method to solve the advection–diffusion equations. For instance, in the aeronautical industry, compressible aerodynamics plays an important role in the design and optimization of new aircraft. In literature, we can find several investigations related to compressible flow. As examples, Sadri *et al.* (2015) use a compact finite difference scheme to solve the compressible Euler equations along with a vorticity method, Xu *et al.* (2018) simulate the transonic flow over the airfoil RAE 2822 in order to analyze the effects of transonic turbulence, Franciolini *et al.* (2018) solve the Navier Stokes equation to analyze the effects of cross flow over an infinite swept wing and Merlin *et al.* (2012) use the LES (large Eddy Simulation) turbulence model along with the a fourth order MacCormack method to simulate the supersonic boundary layer.

2. Methodology

The equations of motion that governs the behavior of a fluid can be derived for the three laws of conservation (conservation of mass, conservation of momentum also known as Newton's second law and conservation of energy). Which, Mathematically can be represented by.

$$\frac{\partial U}{\partial t} + \frac{\partial F}{\partial x} + \frac{\partial G}{\partial y} = J, \tag{1}$$

$$U = \begin{bmatrix} \rho \\ \rho u \\ \rho v \\ \rho\left(e + \frac{\vec{V}^2}{2}\right) \end{bmatrix}, \tag{2}$$

$$F_{inv} = \begin{bmatrix} \rho u \\ \rho u^2 + p \\ \rho uv \\ \rho\left(e + \frac{\vec{V}^2}{2}\right) u + pu \end{bmatrix}, F_{vis} = \begin{bmatrix} 0 \\ \tau_{xx} \\ \tau_{xy} \\ -u\tau_{xx} - v\tau_{xy} - q_x \end{bmatrix}, \tag{3}$$

$$G_{inv} = \begin{bmatrix} \rho v \\ \rho vu \\ \rho v^2 + p \\ \rho\left(e + \frac{\vec{V}^2}{2}\right) v + pv \end{bmatrix}, G_{vis} = \begin{bmatrix} 0 \\ \tau_{yx} \\ \tau_{yy} \\ -u\tau_{xy} - v\tau_{yy} - q_y \end{bmatrix}, \tag{4}$$

$$J = \begin{bmatrix} 0 \\ \rho f_x \\ \rho f_y \\ \rho\left(uf_x + vf_y\right) \end{bmatrix}. \tag{5}$$

The components of the shear stress tensor and are given by:

$$\tau_{xy} = \tau_{yx} = \mu\left(\frac{\partial u}{\partial y} + \frac{\partial v}{\partial x}\right), \tag{6}$$

$$\tau_{xx} = \lambda\left(\frac{\partial u}{\partial x} + \frac{\partial v}{\partial y}\right) + 2\mu\frac{\partial u}{\partial x}, \tag{7}$$

$$\tau_{yy} = \lambda\left(\frac{\partial u}{\partial x} + \frac{\partial v}{\partial y}\right) + 2\mu\frac{\partial v}{\partial y}, \tag{8}$$

The viscosity using the Sutherland law, again assuming a calorically perfect gas.

$$\mu = \mu_0\left(\frac{T}{T_0}\right)^{\frac{3}{2}}\frac{T_0 + 110}{T + 110} \tag{9}$$

2.1 Finite difference compact scheme

High order numerical schemes are better suitable for the analysis of many physical phenomena. In fluid dynamic, compressible flows with generation of shock waves, transition and turbulence inside the boundary layer, flows at high Reynolds, hypersonic flows are examples that require high order of accuracy for get a satisfactory solution. Then, in the compact finite difference approach, the first derivative can be computed by:

$$\beta\phi'_{i-2}+\alpha\phi'_{i-1}+\phi'_i+\alpha\phi'_{i+1}+\beta\phi'_{i+2}= \qquad a\frac{\phi_{i+1}-\phi_{i-1}}{2\Delta x}+b\frac{\phi_{i+2}-\phi_{i-2}}{4\Delta x}+c\frac{\phi_{i+3}-\phi_{i-3}}{6\Delta x} \tag{10}$$

The coefficients a, b, c, α and β are chosen to set the order of accuracy of the stencil with respect with the truncated Taylor series. We are interest in fourth order as maximum for the overall domain, then the values of the coefficient are:$a=\frac{3}{2}, b=0, c=0, \alpha=\frac{1}{4}, \beta=0$. This yield to a tridiagonal system which can be solved employing the Thomas algorithm.

$$\frac{1}{4}\phi_{i-1}+\phi_i+\frac{1}{4}\phi_(i+1)=\frac{3}{4}\frac{\phi_{i+1}-\phi_{i-1}}{\Delta x} \tag{11}$$

Greater orders of accuracy that sixth require a penta-diagonal system, for more detailed information of the coefficients for higher orders the reader may refer to Lele Lele (1992), Visbal and Gaitonde Visbal and Gaitonde (2002), Boersma Boersma (2011) and Lerat Abide *et al.* (2017). In a similar fashion, The second derivative can be computed by.

$$\beta\phi'_{i-2}+\alpha\phi'_{i-1}+\phi'_i+\alpha\phi'_{i+1}+\beta\phi'_{i+2}=a\frac{\phi_{i+1}-\phi_{i-1}}{2\triangle x}+b\frac{\phi_{i+2}-\phi_{i-2}}{4\Delta x}+c\frac{\phi_{i+3}-\phi_{i-3}}{6\Delta x} \tag{12}$$

Equivalently to the first derivative the coefficients are set with the truncated Taylor series.

2.1.1 Boundary conditions for the CFDS

The central stencil in Eq. 11 cannot be applied at the boundary points located at $i=1$ and $i=n$, because one of the points of the stencil lies outside the domain and a new formula is required. Additionally, to maintain the formal order of accuracy of the interior scheme, the stencil at the boundaries has to be adjusted to match the order of accuracy of the interior points. This is done by the next equations:

The first derivative at the boundary at the point i = 1 can be represented by.

$$\phi'_1+\alpha\phi'_2+\beta\phi'_3=\frac{1}{\Delta x}(\phi_1a_1+\phi_2b_1+\phi_3c_1+\phi_4d_1) \tag{13}$$

The coefficients of fourth order of accuracy are:$\alpha=3, \beta=0, a_1=\frac{-17}{6}, b_1=\frac{3}{2}, c_1=\frac{3}{2}, d_1=\frac{-1}{6}$.

Analogously, the first derivative at the boundary point i = n is represented by.

$$\beta_n\phi'_{n-2}+\alpha_n\phi'_{n-1}+\phi'_n=\frac{1}{\Delta x}(\phi_na_n+\phi_{n-1}b_n+\phi_{n-2}c_n+\phi_{n-3}d_n) \tag{14}$$

And the coefficients are: $\alpha_n=3, \beta_n=0, a_n=\frac{17}{6}, b_n=\frac{-3}{2}, c_n=\frac{-3}{2}, d_n=\frac{1}{6}$

2.2 Filtering

In the solution of differential equations by numerical methods, problems like mesh non uniformities, not resolved scales, nonlinearities and boundary con-ditions, can be sources for instabilities. There are two popular approaches to ensuring stability, adding some amount of damping (or artificial viscosity) or by filtering. We focus our attention in the study of filtering. We focus our attention in the study of filtering, in literature there are several types of filters, for instance bogey and balli present a family of low dissipative explicit filters, while Lele (1992) and Visbal and Gaitonde (2002) presents a variety of implicit filters. In this paper an implicit filter is used. The filtering task requires that the computed variables ϕ or the solution vector U which can be computed the following equation.

$$\alpha f\overline{\phi}_{i-1}+\overline{\phi}_i+\alpha f\overline{\phi}_{i+1}=\sum_{n=0}^{N}\frac{a_n}{2}(\phi_{i+n}-\phi_{i-n}) \tag{15}$$

2.3 Immersed Interface Boundary Method

This method is similar to the approximations used in Linnick and Fasel (2005), Hosseinverdi and Fasel and Marichal *et al.* (2016).

2.3.1 Correction of the Taylor Series for discontinuous functions

Due the discontinuities across the boundary interface. The standard Taylor series cannot be applied because this is not valid through singularities, then the Taylor series must be corrected in order to maintain the accuracy of the method, for the function and his derivatives.

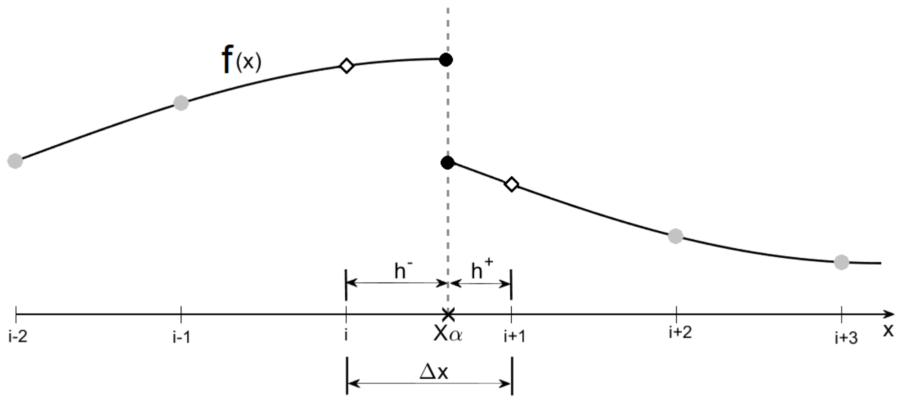

Figure 1: Discontinouns function at x_α

For this especial case the Taylor series around x i can be expressed as follow:

$$f_{i+1} = f_i + f'\Delta x + f''\frac{\Delta x^2}{2!} + f'''\frac{\Delta x^3}{3!} + ... + J_\alpha \tag{16}$$

Where J_α is called jump correction term and is given by.

$$J_\alpha = [f]_\alpha + [f']_\alpha h^+ + [f'']_\alpha \frac{(h^+)^2}{2!} + [f''']_\alpha \frac{(h^+)^3}{3!} \tag{17}$$

$\Delta x = x_{i+1} + x_i$ and $h^+ = x_{i+1} - x_\alpha$. The terms $[*]_\alpha$ represent the jumps in the function of Eq. 16.

2.3.2 Finite difference scheme with jump correction

In the finite difference method, any derivative can be replaced by a similar differential quotients, using the Taylor series expansion

$$f' = R_{i-1}f_{i-1} + R_iF_{i-1} + R_{i+1}f_{i+1} + R_{i+1}J_\alpha \tag{18}$$

and

$$f'' = R_{i-1}f_{i-1} + R_if_{i-1} + R_{i+1}f_{i+1} + R_{i+1}J_\alpha \tag{19}$$

2.3.3 Jump correction term

With reference to Fig. 1, for the interface x_α between x_i and x_{i+1} , the spacing $h^+ = x_{i+1} - x_\alpha$ and

$$J_{\alpha k} = \sum_{n=k}^{N} [f^n]_\alpha \frac{h^{(n-k)}}{(n-k)!} \tag{20}$$

If the interface x_α lies between x_{i1} and x_i , the spacing $h^- = x_\alpha - x_{i1}$ and

$$J_{\alpha k} = \sum_{n=k}^{N} -1^{(n-k+1)}[f^n]_\alpha \frac{h^{(n-k)}}{(n-k)!} \tag{21}$$

The jumps $[f^n]_\alpha$ are given by:

$$[f^n]_\alpha = f^n_{F.D^+} - f_{F.D^-} \tag{22}$$

Where

$$f^n_{F.D^+} = c^+_\alpha f^+_\alpha \sum_{k=1}^{N} c^n_k f_{i+k-1} \tag{23}$$

And

$$f^n_{F.D^+} = c^-_\alpha f^-_\alpha \sum_{k=1}^{N} c^n_k f_{i-k+1} \tag{24}$$

Where the spacing $h_i = x_\alpha - x_i$ and $\delta_{i,j}$ is the Kronecker delta defined by.

$$\delta_{i,j} = \begin{cases} 1 & If\ i = j \\ 0 & If\ i \neq j \end{cases} \tag{25}$$

2.3.4 Compact scheme for the IIB Method

In order to apply the IIB together with the compact scheme, we replace the spatial derivatives of Eq. 1 $\frac{\partial F}{\partial x}$ and $\frac{\partial G}{\partial y}$ as follow. Second derivatives also is presented, due her use in the validation section.

$$L_{i-1}f'_{i-1} + L_i f'_i + L_{i+1}f'_{i+1} = R_{i-1}f_{i-1} + R_i f_i + R_{i+1}f_{i+1} - (L_1 J_{\alpha 1} - R_1 J_{\alpha 0}) \tag{26}$$

For second derivative.

$$L_{i-1}f''_{i-1} + L_i f''_i + L_{i+1}f''_{i+1} = R_{i-1}f_{i-1} + R_i f_i + R_{i+1}f_{i+1} - (L_1 J_{\alpha 2} - R_1 J_{\alpha 0}) \tag{27}$$

If the jump singularity lies between $x_i < x_\alpha < x_{i+1}, h^+ = x_{i+1} - x_\alpha$

$$J_{\alpha 0} = [f]_\alpha + [f']_\alpha h^+ + [f'']_\alpha \frac{(h^+)^2}{2!} + [f''']_\alpha \frac{(h^+)^3}{3!} + [f'''']_\alpha \frac{(h^+)^4}{4!} + [f''''']_\alpha \frac{(h^+)^5}{5!} \tag{28}$$

$$J_{\alpha 1} = [f']_\alpha + [f'']_\alpha h^+ + [f'']_\alpha \frac{(h^+)^2}{2!} + [f''']_\alpha \frac{(h^+)^3}{3!} + [f'''']_\alpha \frac{(h^+)^4}{4!} \tag{29}$$

$$J_{\alpha 2} = [f'']_\alpha + [f''']_\alpha h^+ + [f'''']_\alpha \frac{(h^+)^2}{2!} + [f''''']_\alpha \frac{(h^+)^3}{3!} \tag{30}$$

If the jump singularity lies between $x_{i1} < x_\alpha < x_i, h^{=x_\alpha x_{i1}}$

$$J_{\alpha 0} = -[f]_\alpha + [f']_\alpha h^- - [f'']_\alpha \frac{(h^-)^2}{2!} + [f''']_\alpha \frac{(h^-)^3}{3!} - [f'''']_\alpha \frac{(h^-)^4}{4!} + [f''''']_\alpha \frac{(h^-)^5}{5!} \tag{31}$$

$$J_{\alpha 1} = -[f']_\alpha + [f'']_\alpha h^- + [f''']_\alpha \frac{(h^-)^2}{2!} + [f'''']_\alpha \frac{(h^-)^3}{3!} - [f'''']_\alpha \frac{(h^-)^4}{4!} \tag{32}$$

$$J_{\alpha 2} = -[f'']_\alpha + [f''']_\alpha h^- + [f'''']_\alpha \frac{(h^-)^2}{2!} + [f''''']_\alpha \frac{(h^-)^3}{3!} \tag{33}$$

3. Validation and Verification

3.1 Two dimensions

In two dimensional form Eq. 34 is represented by:

$$\frac{\partial \phi}{\partial t} = \mu_x \frac{\partial^2 \phi}{\partial x^2} + \mu_y \frac{\partial^2 \phi}{\partial y^2} - u_x \frac{\partial \phi}{\partial x} - u_y \frac{\partial \phi}{\partial y} \tag{34}$$

The domain is located in the interval [02]x[02], discretized with a regular equal spacing mesh in both directions with a number of grid nodes $nx = ny =$ [40, 80, 160, 320, 640] the spacing is given by $\Delta x = \frac{L_x}{nx-1}$ and $\Delta y = \frac{L_y}{ny-1}$, the values of the diffusion coefficients are μ_x = 0.01 and μ_x= 0.01, and the advection speeds are u_x = 0.1 and u_y = 0.1, the boundary conditions at x = 0, x = 2, y = 0 and y = 2 are Dirichlet and set equal to zero, the step size is constant and equal to 2.5e-3. The simulation time is 0.625 [sg] with a dt = $5e\ \ 5[sg]$. The analytical solution is given by:

$$\phi_{(t,x,y)} = \frac{1}{4t+1}\left(\frac{(x-u_x t-0.5)^2}{\mu_x(4t+1)} - \frac{(y-v_x t-0.5)^2}{\mu_y(4t+1)}\right) \tag{35}$$

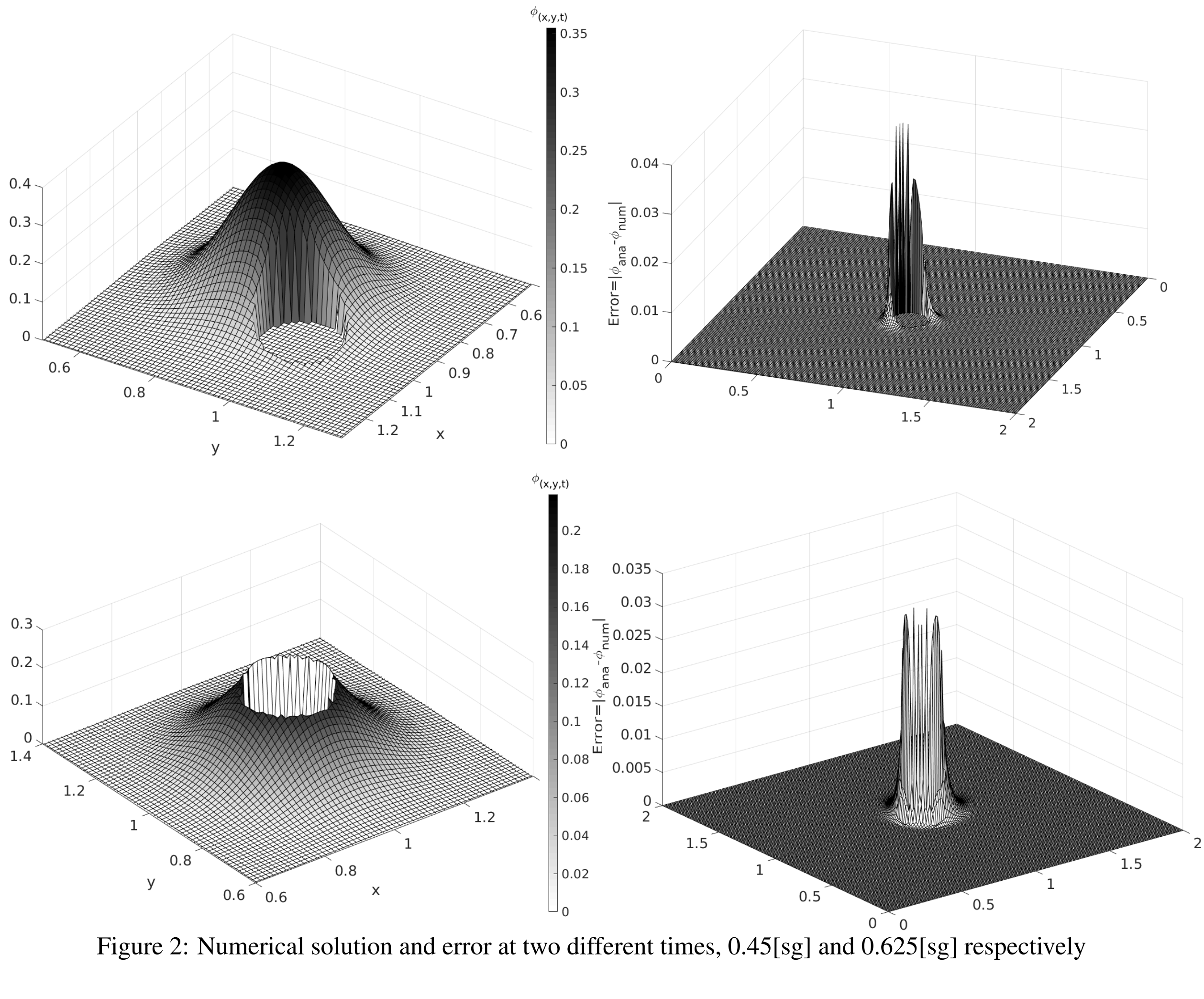

Figure 2: Numerical solution and error at two different times, 0.45[sg] and 0.625[sg] respectively

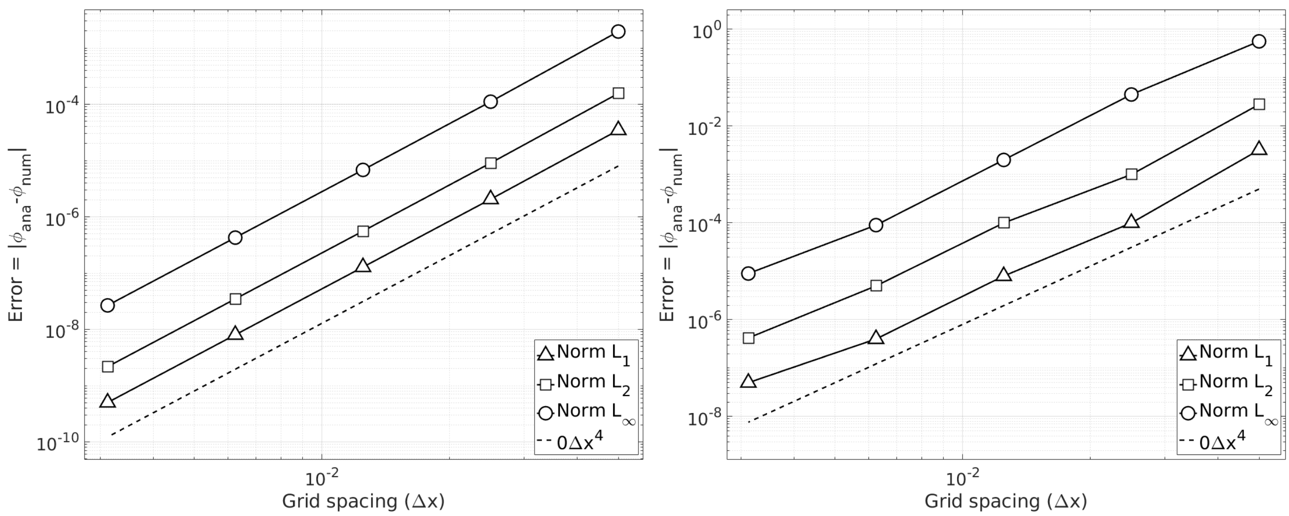

Figure 3: Convergence rate as a function of the grid spacing Δ_x using the norms L_1 ,L_2 and $L\infty$. Fourth order of convergence is indicated (one dimensional case)

3.2 Supersonic flow over a flat plate

The viscous compressible supersonic flow over a flat plate is used as an example to verificate the code. Consider a rectangular domain with dimensions $Lx = 0.00001[m]$ and $Ly = 5\delta[m]$, where $\delta = \frac{5Lx}{\sqrt{Re_l}}$ and Re_l is the Reynolds number at the end of the plate, the domain is discretized with a number of grid points $nx = ny = 100$, in the x direction the grid is regular with equal spacing given by $\Delta x = \frac{L_x}{nx-1}$, while in the y direction the mesh stretched, given by the function.

$$y(j) = L_y \frac{(\beta+1)-(\beta-1)(\frac{\beta+1}{\beta-1})^{1-\frac{j-1}{my-1}}}{(\frac{\beta+1}{\beta-1})^{1-\frac{j-1}{my-1}}+1} \tag{36}$$

j is the index in the y direction, $j = 1$ at $y = 0$ and $j = my$ at $y = Ly$, β is a parameter to control the stretch of the grid. As initial condition the flow properties are set as ISA(International standard atmosphere) see level condition, speed of sound $a = 340.28[m/s]$, pressure $p = 101325[N/m2]$, temperature $T = 288.16[k]$, specific get relationship $\gamma = 1.4$, dynamic viscosity $\mu = 1.7894X10^5 kg/(msg)$, specific gas constant $287J/(Kg*K)$ at a free stream Mach number $M = 4.0$. The boundary conditions set as Dirichlet with the value of the free stream at the inlet, and for the outlet all variables are set as Neumann, with his derivatives equal to zero. Here the mesh is treated like a fluid and the embedded body (the flat plate or Lagrangian mesh) is located at $0.7\Delta y_1$ where $\Delta y_1 = y_2 - y_1$ at the surface of the plate, no slip boundary condition is enforced with the velocity components $u = v = 0[m/s]$, the temperature is Dirichlet for the isothermal case ($T = T_\infty$) and Neumann for the adiabatic case $\frac{dT}{dy} = 0$, the pressure is set as Neumann $\frac{dp}{dy} = 0$. The code runs until achieving the steady state solution, the convergence of the solution is assumed when the residual reaches a target value of 10^5 , in Fig.4 show the residual of three variables (pressure, density and velocity) they all reach the desired target.

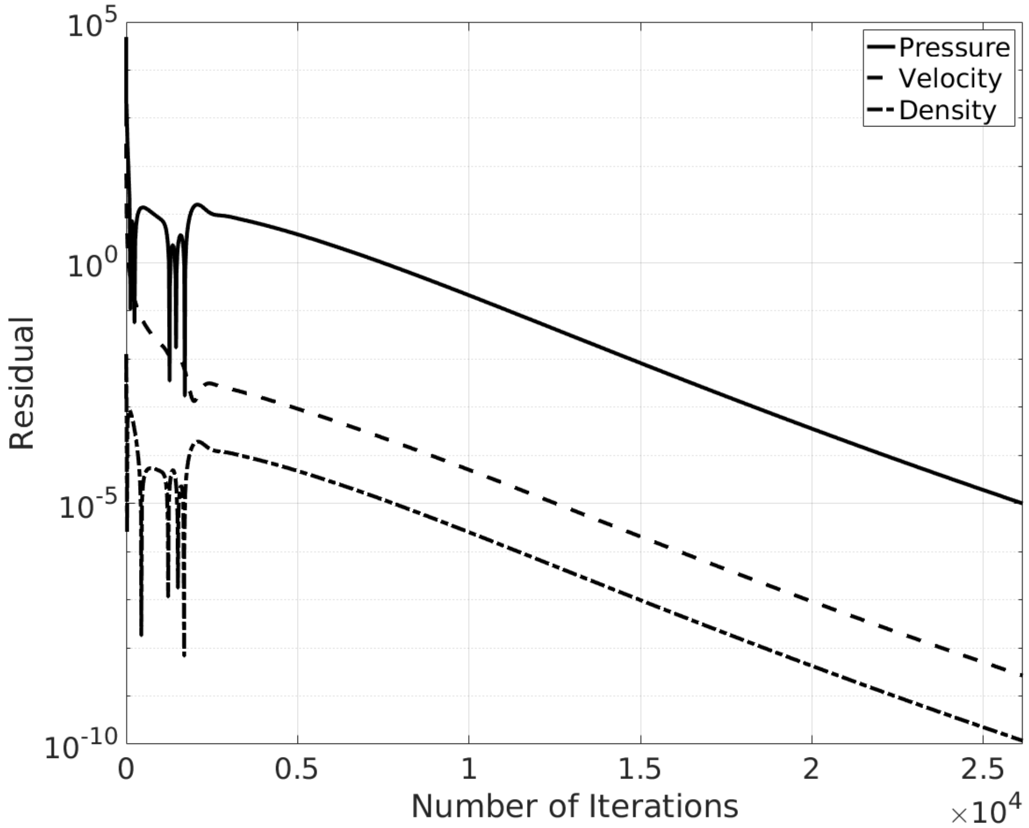

Figure 4: Monitor of the residual of the variables pressure, velocity and density

Fig.5 present the results at the outlet, with the distance in the y direction normalized by the equation $y_n = \frac{y}{x}\sqrt{Re}$ and the adimensional values of pressure, temperature and velocity for an isothermal and adiabatic flow, the IIM is compared with the results from Anderson (1995). All three profiles pressure, temperature and velocity are similar to the presented by Anderson (1995). The fields for pressure, temperature and velocity for the steady state solution are represented in Fig.6 and Fig.7.

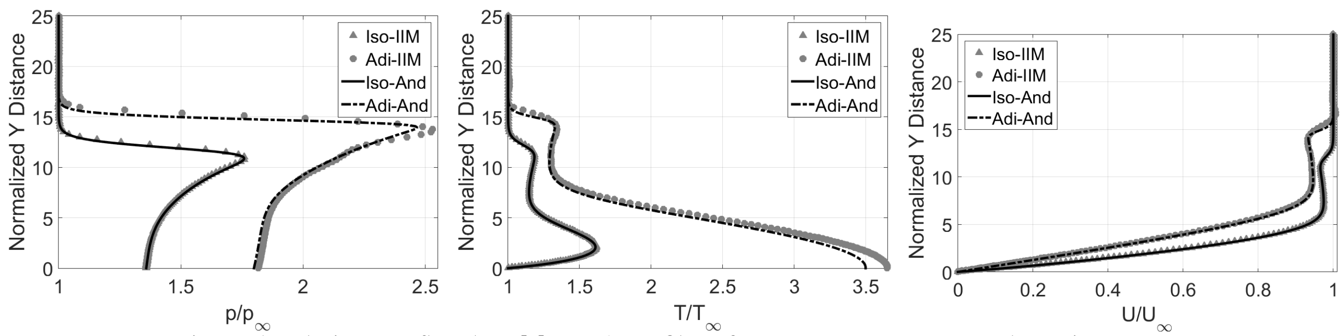

Figure 5: solution at a flat plate $M_\infty = 4$, profiles of pressure, temperature and veocity

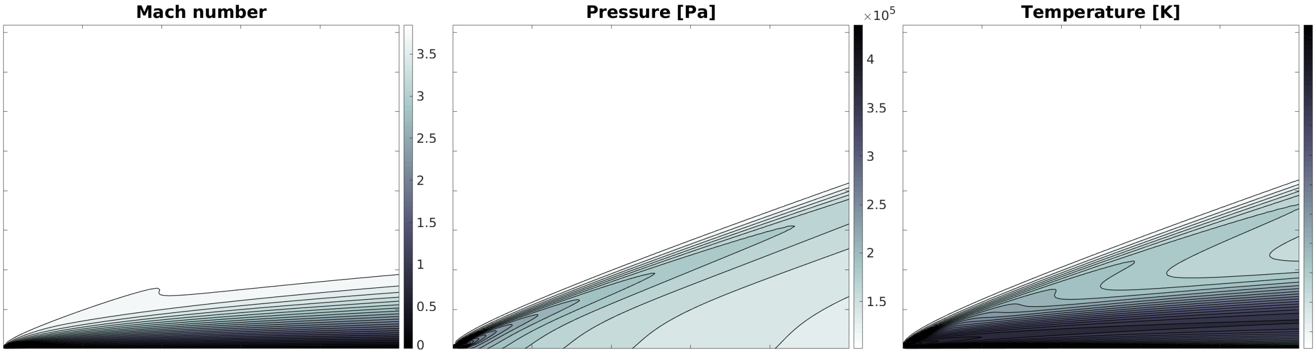

Figure 6: steady state solution for the flat plate at $M_\infty = 4.0$, Mach number, pressure and temperature field respectively, isotermal case

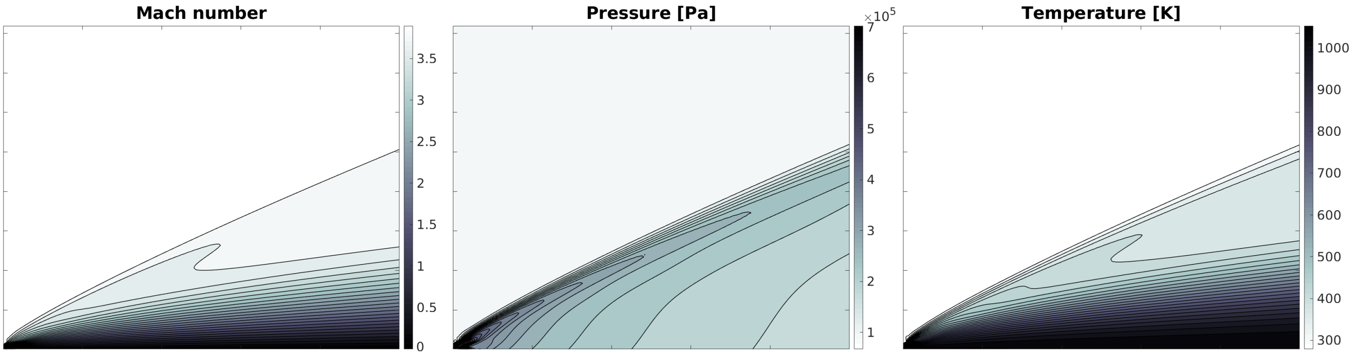

Figure 7: steady state solution for the flat plate at $M_\infty = 4.0$, Mach number, pressure and temperature field respectively, adiabatic case

4. Conclusions

The IIM presented in this paper for compressible flows, presents good agreement between the analytical result and other numerical results in the validation and verification section. The order of accuracy was proved to be fourth with the use of the advection diffusion equation in one and two dimensions, also the results of the supersonic flow over the flat plate are similar to other numerical results.

5. REFERENCES

Abide, S., Binous, M. and Zeghmati, B., 2017. "An efficient parallel high-order compact scheme for the 3D incompressible Navier–Stokes equations". *International Journal of Computational Fluid Dynamics*, pp. 1–16. doi: 10.1080/10618562.2017.1326592.

Anderson, J.D., 1995. *Computational Fluid Dynamics: The Basics with Applications*. McGraw-Hill international editions. McGraw-Hill.

Boersma, B.J., 2011. "A 6th order staggered compact finite difference method for the incompressible Navier-Stokes and scalar transport equations". *J. Comput. Physics*, Vol. 230, pp. 4940–4954. doi:10.1016/j.jcp.2011.03.014.

Franciolini, M., Da Ronch, A., Drofelnik, J., Raveh, D. and Crivellini, A., 2018. "Efficient infinite-swept wing solver for steady and unsteady compressible flows". *Aerospace Science and Technology*, Vol. 72, pp. 217–229. ISSN 1270-9638. doi:https://doi.org/10.1016/j.ast.2017.10.034. URL `https://www.sciencedirect.com/science/article/pii/S1270963817303905`.

Goldstein, D., handler, R. and Sirovich, L., 1993. "modelling a no slip flow boundary with an external force field". *Journal of Computational Physics*, Vol. 105, No. 2, pp. 354–366.

Hossan, M.R., Dillon, R. and Dutta, P., 2014. "Hybrid immersed interface-immersed boundary methods for AC dielectrophoresis". *Journal of Computational Physics*, Vol. 270, pp. 640–659. ISSN 0021-9991. doi:https://doi.org/10.1016/j.jcp.2014.04.012. URL `https://www.sciencedirect.com/science/article/pii/S0021999114002757`.

Hosseinverdi, S. and Fasel, H.F., ???? *Very High-Order Accurate Sharp Immersed Interface Method: Application to Direct Numerical Simulations of Incompressible Flows*. doi:10.2514/6.2017-3624. URL `https://arc.aiaa.org/doi/abs/10.2514/6.2017-3624`.

Hu, W.F., Lai, M.C. and Young, Y.N., 2015. "A hybrid immersed boundary and immersed interface method for electrohydrodynamic simulations". *Journal of Computational Physics*, Vol. 282, pp. 47–61. ISSN 0021-9991. doi:https://doi.org/10.1016/j.jcp.2014.11.005. URL https://www.sciencedirect.com/science/article/pii/S0021999114007578.

Lai, M.C. and Li, Z., 1999. "A Remark on Jump Conditions for the Three-Dimensional Navier-Stokes Equations Involving an Immersed Moving Membrane". *Applied Mathematics Letters*, Vol. 12, pp. 7–11.

Lele, S.K., 1992. "Compact finite difference schemes with spectral-like resolution". *Journal of Computational Physics*, Vol. 103, No. 1, pp. 16–42. ISSN 0021-9991. doi:https://doi.org/10.1016/0021-9991(92)90324-R. URL https://www.sciencedirect.com/science/article/pii/002199919290324R.

Li, Z. and Ito, K., 2006. *The Immersed Interface Method*. Society for Industrial and Applied Mathematics. doi: 10.1137/1.9780898717464. URL https://epubs.siam.org/doi/abs/10.1137/1.9780898717464.

Linnick, M.N. and Fasel, H.F., 2005. "A high-order immersed interface method for simulating unsteady incompressible flows on irregular domains". *Journal of Computational Physics*, Vol. 204, No. 1, pp. 157–192. ISSN 0021-9991. doi:https://doi.org/10.1016/j.jcp.2004.09.017. URL https://www.sciencedirect.com/science/article/pii/S0021999104004127.

Marichal, Y., Chatelain, P. and Winckelmans, G., 2016. "Immersed interface interpolation schemes for particle–mesh methods". *Journal of Computational Physics*, Vol. 326, pp. 947–972. ISSN 0021-9991. doi:https://doi.org/10.1016/j.jcp.2016.09.027. URL https://www.sciencedirect.com/science/article/pii/S0021999116304417.

Merlin, C., Domingo, P. and Vervisch, L., 2012. "Immersed Boundaries in Large Eddy Simulation of Compressible Flows". *Flow, Turbulence and Combustion*, Vol. 90, No. 1, pp. 29–68.

Mohd-yusof, 1997. "Combined immersed-boundary / B-spline methods for simulations of ow in complex geometries". *Center for Turbulence Research Annual Research Briefs*, pp. 317–327.

Peskin, C.S., 1977. "Numerical analysis of blood flow in the heart". *Journal of Computational Physics*, Vol. 25, No. 3, pp. 220–252.

Peskin, C.S., 2003. "The immersed boundary method". *Acta Numerica*, Vol. 11, pp. 479–517.

Sadri, M., Hejranfar, K. and Ebrahimi, M., 2015. "On application of high-order compact finite-difference schemes to compressible vorticity confinement method". *Aerospace Science and Technology*, Vol. 46, pp. 398–411. ISSN 1270-9638. doi:https://doi.org/10.1016/j.ast.2015.07.023. URL https://www.sciencedirect.com/science/article/pii/S1270963815002370.

Sciences, A.E., 1996. "Numerical Simulation of a Cylinder in Uniform Flow : Application of a Virtual Boundary Method". Vol. 465, No. 123, pp. 450–465.

Solarte-Pineda, J. and Greco, P.C., 2016. "Virtual boundary method for inviscid transonic flow over supercritical airfoils". *Aerospace Science and Technology*, Vol. 58, pp. 380–388. ISSN 1270-9638. doi:https://doi.org/10.1016/j.ast.2016.08.024. URL https://www.sciencedirect.com/science/article/pii/S1270963816305120.

Visbal, M.R. and Gaitonde, D.V., 2002. "On the Use of Higher-Order Finite-Difference Schemes on Curvilinear and Deforming Meshes". *Journal of Computational Physics*, Vol. 181, No. 1, pp. 155–185. ISSN 0021-9991. doi:https://doi.org/10.1006/jcph.2002.7117. URL https://www.sciencedirect.com/science/article/pii/S0021999102971172.

Xu, J., Chen, D., Song, Y., Ji, S. and Zhou, Y., 2018. "Mean flow compressibility effects in transonic turbulence modeling". *Aerospace Science and Technology*, Vol. 79, pp. 492–499. ISSN 1270-9638. doi:https://doi.org/10.1016/j.ast.2018.06.005. URL https://www.sciencedirect.com/science/article/pii/S1270963817321557.

Xu, S., 2011. "A boundary condition capturing immersed interface method for 3D rigid objects in a flow". *Journal of Computational Physics*, Vol. 230, No. 19, pp. 7176–7190. doi:10.1016/j.jcp.2011.05.019.